Chapter 61
Research on the Effect of Code Doppler on Acquisition Performance and the Compensation Methods

Linfeng Zhang, Tianqiao Zhang, Hong Li, Xiaowei Cui and Minquan Lu

Abstract The relative motion between the navigation satellites and receivers not only brings carrier Doppler (CAD) but also code Doppler (COD). Under a strong signal circumstance, the pre-detection integration time (PIT) is short and only the CAD is needed to be considered, while in the weak signal environments, in order to accumulate more signal energy, the PIT has to be extended. During the extension of PIT, the code autocorrelation function suffers attenuation, displacement and broadening by COD, which should be compensated. This paper studied the impacts of COD on acquisition performance such as sensitivity and availability, and then introduced some existing compensation methods of COD. After investigating the strengths and weaknesses of the existing methods, a new compensation method was proposed, which compensated COD at the stages of down-sampling and non-coherent accumulation (NCA). Different methods were evaluated on a software platform, and testing results proved the superiority of the new method.

Keywords Weak signal · Code doppler · Spread-spectrum code acquisition

61.1 Introduction

With the widespread applications of Global Navigation Satellite System (GNSS) receivers, the newer and more challenging environments, such as indoor, forest and urban, ask for higher acquisition sensitivity [1]. In order to improve the

L. Zhang (✉) · H. Li · X. Cui · M. Lu
Department Electronic Engineering, Tsinghua University,
1110 Wei Qing Building, Beijing, P. R. China
e-mail: zhanglinf04@gmail.com

T. Zhang
Beijing Satellite Navigation Center, Beijing, P. R. China

J. Sun et al. (eds.), *China Satellite Navigation Conference (CSNC) 2013 Proceedings*, Lecture Notes in Electrical Engineering 243,
DOI: 10.1007/978-3-642-37398-5_61,

acquisition sensitivity, it's necessary to extend the PIT to accumulate more signal energy [2]. During this process, by the COD influence, the code autocorrelation function suffers attenuation, displacement and broadening [3], which attenuates the accumulation of signal energy. To solve this problem, a compensation for COD is essential. In literature [4–6], COD is compensated by adjusting the generating rate of local code. This method is simple and intuitive, but the local code sequences has to be updated frequently, which increases the calculation, and the extension of PIT is restricted by the residual code Doppler (RCOD). In literature [7], Code Doppler is compensated in the procedure of NCA by shifting the coherent integration results. This method avoids updating local code frequently, but the shifting operation reduces the autocorrelation peak, and the PIT is also limited by RCOD. In this paper, a novel method is proposed and the compensation is implemented in processes of down-sampling and NCA.

The paper is organized as follows: Sect. 61.2 analyzes the impact of COD on acquisition performance. Section 61.3 introduces the main existing compensation methods and summarizes their strengths and weaknesses. In Sect. 61.4 a novel compensation method is proposed. Section 61.5 presents and analyzes the test results of different methods. Finally, in Sect. 61.6 some conclusions are drawn.

61.2 Effect of Code Doppler on Acquisition Performance

Figure 61.1 shows the pre-detection integration flow of GNSS acquisition module (only code component is considered), in which the input signal is

$$S_1(k) = C[(1+\eta)kT_s - \tau] \tag{61.1}$$

where $C(t)$ is the received PRN code, τ is the code delay, T_s is the sampling interval, $\eta = f_{D,c}/f_c = f_D/f_{RF}$ is the code-phase drift rate and $f_{D,c}$ and f_D are the COD and CAD respectively, f_c and f_{RF} are the nominal code rate and carrier frequency, respectively.

The expression of coherent integration result in Fig. 61.1 is

$$S_2 = \sum_{k=1}^{K} C[(1+\eta)kT_s - \tau]C[kT_s - \hat{\tau}] = R\left(\Delta\tau, T_{coh}, f_{D,c}\right) \tag{61.2}$$

where T_{coh} is the length of coherent integration time,K is the number of samples in T_{coh}, $\hat{\tau}$ is the local code delay and $\Delta\tau = \tau - \hat{\tau}$. Actually, S_2 is the code correlation

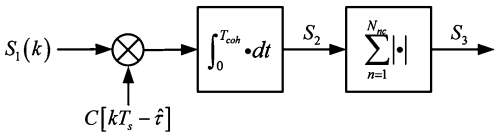

Fig. 61.1 Pre-detection integration flow of acquisition module

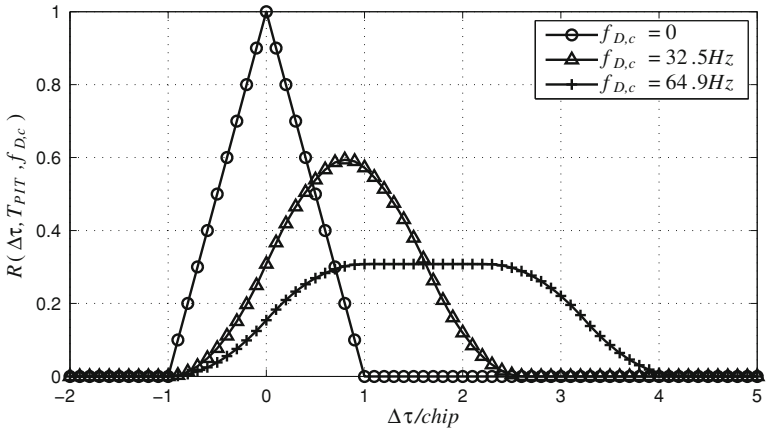

Fig. 61.2 Code Autocorrelation function under different COD

function which considers COD and its formula can be found in literature [3, 8]. The value of S_2 is determined by $\Delta\tau$, T_{coh} and $f_{D,c}$, so we also express it as $R\left(\Delta\tau, T_{coh}, f_{D,c}\right)$.

After the procedure of NCA, we get

$$S_3 = \sum_{n=1}^{N_{nc}} R\left(\Delta\tau_n, T_{coh}, f_{D,c}\right) = R\left(\Delta\tau, T_{PIT}, f_{D,c}\right) \tag{61.3}$$

where N_{nc} is the number of NCA, $\Delta\tau_n = \Delta\tau + (n-1)\eta T_{coh}$, and $T_{PIT} = N_{nc}T_{coh}$.

Figure 61.2 shows the code autocorrelation function under different COD, in which $T_{coh} = 1$ ms, $N_{nc} = 50$ and $f_c = 10.23$ MHz. From Fig. 61.2 we can see that the code autocorrelation peak suffers attenuation, displacement and broadening when $f_{D,c} \neq 0$. The formulas of attenuation ratio, shifting distance and the peak width are as follows [3]:

$$L_p(\Delta p) = \begin{cases} (1 - 0.25|\Delta p|)^{-2}, & |\Delta p| \leq 2 \\ (\Delta p)^2, & |\Delta p| > 2 \end{cases} \tag{61.4}$$

$$S_p(\Delta p) = \Delta p/2 \tag{61.5}$$

$$W_p(\Delta p) = 2 + |\Delta p| \tag{61.6}$$

where $\Delta p = f_{D,c}T_{PIT}$ is the relative sliding code-phase between the received code and the local code during T_{PIT} in number of chips. The attenuation of correlation peak will affect the acquisition sensitivity, while the shifting and broadening of correlation peak will reduce the availability of acquisition results.

61.2.1 Effect on Acquisition Sensitivity

To facilitate the derivation, it is assumed that the object of NCA is power rather than amplitude, then S_3 can be written as

$$S_3' = \sum_{n=1}^{N_{nc}} R^2\left(\Delta\tau_n, T_{coh}, f_{D,c}\right)/\sigma^2 \tag{61.7}$$

where σ^2 is the noise variance of coherent integration result. Then the attenuation ratio in Eq. (61.4) becomes

$$L_p' = N_{nc}R^2(0, T_{coh}, 0)/\sum_{n=1}^{N_{nc}} R^2\left(\Delta\tau_n, T_{coh}, f_{D,c}\right) \tag{61.8}$$

where $\Delta\tau_n = \Delta p/2 + (n-1)\eta T_{coh}$ and $\Delta p/2$ is the position of summit in Fig. 61.2.

When signal is absent, S_3' is distributed according to the Chi square distribution and the probability density function (PDF) is

$$f_A(x;k) = \frac{x^{k/2-1}e^{-x/2}}{2^{k/2}\Gamma(k/2)} \tag{61.9}$$

where $\Gamma(n) = (n-1)!$ is the Gama function and $k = 2N_{nc}$ is the degrees of freedom.

Then the false alarm probability of acquisition is

$$P_{fa} = \int_{x=V_t}^{+\infty} f_A(x;k)dx \tag{61.10}$$

where V_t is the detection threshold.

S_3' is distributed according to the noncentral Chi squared distribution when signal is present and the corresponding PDF is

$$f_D(x;k,\lambda) = \frac{1}{2}e^{-(x+\lambda)/2}(x/\lambda)^{k/4-1/2}I_{k/2-1}(\lambda x) \tag{61.11}$$

where $I_v(z)$ is a modified Bessel function of the first kind, λ is the noncentrality parameter and can be written as

$$\lambda = \sum_{n=1}^{N_{nc}} \left(\frac{a_n}{\sigma}\right)^2 = \sum_{n=1}^{N_{nc}} SNR_n = C/N_0 \times T_{PIT}/L_p' \tag{61.12}$$

where a_n^2 and SNR_n are the signal power and the signal noise ratio of the nth coherent integration result, respectively. C/N_0 is the carrier to noise ratio. Then the final detection probability is

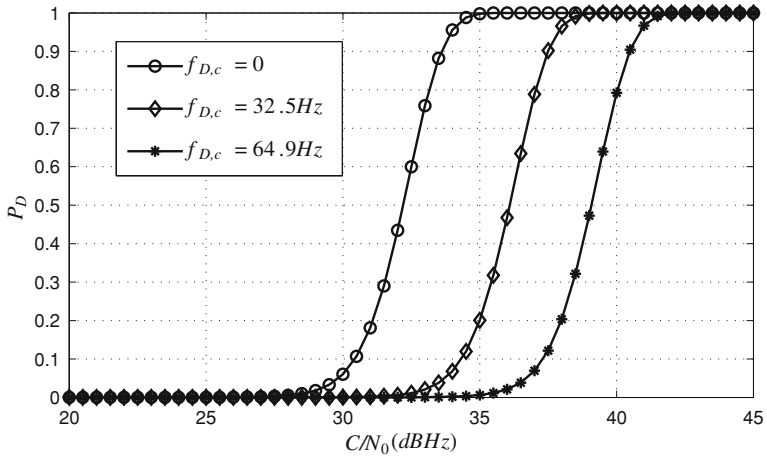

Fig. 61.3 C/N_0 versus P_D under different COD (P_{fa} = 1e-6)

$$P_D = Q_{N_{nc}}\left(\sqrt{\lambda},\ \sqrt{V_t}\right) \tag{61.13}$$

where $Q_n(\cdot,\cdot)$ is the Marcum's Q-function. From the above expressions we can find that when P_{fa} and T_{PIT} are constant, the larger $\left|f_{D,c}\right|$ is, the lower P_D is, and the lower acquisition sensitivity is. The curve of C/N_0 versus P_D under different COD is shown in Fig. 61.3 when $P_{fa} = 1e\text{-}6$ and other parameters are the same as Fig. 61.2. In Fig. 61.3, the losses of sensitivity are 3.9 and 6.9 dB, respectively, when $f_{D,c} = 32.5$ Hz and $f_{D,c} = 64.9$ Hz. This part of sensitivity loss is not acceptable in the weak signal conditions and must be compensated.

61.2.2 Effect on Acquisition Results Availability

In this section we define the code-phase error as $\Delta p_0 = p - p_0$, where p is the code-phase reported after a successful acquisition, p_0 is the real code-phase at the beginning of integration. From Eq. (61.5) and (61.6) we know that the distribution of Δp_0 is

$$\Delta p_0 \sim \begin{cases} U[-0.25 + 0.5\Delta p,\ \ 0.25 + 0.5\Delta p], & |\Delta p| \le 2.5 \\ U[1,\ \ \Delta p - 1], & \Delta p > 2.5 \\ U[1 + \Delta p,\ \ -1], & \Delta p < -2.5 \end{cases} \tag{61.14}$$

To ensure the availability of p, Δp_0 should fall within the pull-in scope of discriminator. When the pull-in scope is ± 0.5 chip, by Eq. (61.14) we can deduce that

$$P(-0.5 \le \Delta p_0 \le 0.5) = \begin{cases} 1, & |\Delta p| < 0.5 \\ 1.5 - |\Delta p|, & 0.5 \le |\Delta p| \le 1.5 \\ 0, & |\Delta p| > 1.5 \end{cases} \tag{61.15}$$

It can be drawn from the above formula that the acquisition result is not available at all if $|\Delta p| > 1.5$, which is easily to meet with the extension of T_{PIT}. So the COD needs to be compensated to guarantee the availability of acquisition results.

61.3 The Existing Compensation Methods

There are two main existing COD compensation methods. The first one is to adjust the generation rate of local code according to the CAD hypothesis [4–6] (referred to as method A hereinafter), and the second one is to shift the coherent integration results before NCA [7] (referred to as method B hereinafter). The two methods are briefly described below.

61.3.1 Method A

In method A the expression of local code samplings is $C[(1+\hat{\eta})kT_s - \hat{\tau}]$, where $\hat{\eta} = \hat{f}_D / f_{RF}$ and $\hat{f}_D$ is the hypothetical CAD. Since the value of $\hat{\eta}$ is not constant, the local code samplings need to be updated frequently, which increases the calculations. The results of coherent integration and NCA are

$$\begin{cases} S_{2,A} = R\left(\Delta\tau, T_{coh}, \Delta f_{D,c}\right) \\ S_{3,A} = R\left(\Delta\tau, T_{PIT}, \Delta f_{D,c}\right) \end{cases} \tag{61.16}$$

where $\Delta f_{D,c} = (\eta - \hat{\eta}) f_c$ is the RCOD and its distribution is

$$\Delta f_{D,c} \sim U[-\Delta f_D f_c / (2 f_{RF}), \quad \Delta f_D f_c / (2 f_{RF})] \tag{61.17}$$

where Δf_D is the search interval of CAD.

The extension of T_{PIT} is limited when $\Delta f_D \neq 0$. By Eq. (61.15) we can infer that the next inequality must be satisfied to ensure the availability of acquisition results.

$$T_{PIT} \le f_{RF} / (\Delta f_D f_c) \tag{61.18}$$

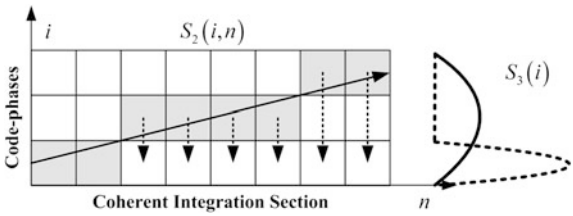

Fig. 61.4 Diagram of shifting NCA of method B

61.3.2 Method B

The principle of NCA in method B is illustrated in Fig. 61.4, in which i and n are the index of code-phases and coherent integration period respectively, the gray grids show the trace of correlation peak. The formula of NCA in Fig. 61.4 is

$$S_{3,B}(i) = \sum_{n=1}^{N_{nc}} S_2\left(i - \left[\left[\hat{f}_{D,c}(n-1)T_{coh}/\tau_s\right]\right],\ n\right) = \sum_{n=1}^{N_{nc}} R\left(\Delta\tau(i,n), T_{coh}, f_{D,c}\right) \tag{61.19}$$

where τ_s is the search step of code-phase, $\hat{f}_{D,c} = \hat{f}_D f_c / f_{RF}$ is the hypothetical COD, $[\![\cdot]\!]$ represents rounding to the nearest integer and

$$\Delta\tau(i,n) = \Delta\tau_i - \tau_s T_c \left[\left[\hat{f}_{D,c}(n-1)T_{coh}/\tau_s\right]\right] + (n-1)f_{D,c}T_{coh}/f_c \tag{61.20}$$

where $\Delta\tau_i = p_i - p_0$ and p_i is the ith code-phase.

The rounding operation in Eq. (61.19) will bring some loss to correlation peak. The average loss of correlation peak is about 0.3 dB when $\hat{f}_{D,c} = f_{D,c}$, $T_{coh} = 1$ ms and $N_{nc} = 500$. From the above formulas we find that the extension of T_{PIT} is also restricted by the RCOD in method B.

61.4 A New Compensation Method

This section presents a novel method (referred to as method C hereinafter), in which COD is compensated at two-stage. The first stage is achieved by adjusting the down-sampling rate according to the hypothetical CAD while keeping the sampling rate of local code unchanged, thus avoids the frequent update of local code samplings. In order to support a longer T_{PIT}, the second stage is carried out during NCA by hypothesis testing the RCOD.

The down-sampling interval of method C is

$$T_s' = T_s(1+\hat{\eta}) = T_s/\left(1+\hat{f}_D/f_{RF}\right) \tag{61.21}$$

By substituting Eq. (61.21) into Eq. (61.2), the coherent integration result is

$$S_{2,C} = R\left(\Delta\tau_0, T_{coh}, \Delta f_{D,c}\right) \tag{61.22}$$

In order to compensate the unknown $\Delta f_{D,c}$, we test a number of hypotheses for $\Delta f_{D,c}$. The mth hypothesis of $\Delta f_{D,c}$ is

$$\Delta f_{D,c,m} = \left(\left[2(m-1) + 1 - M\right]\Delta f_D f_c\right)/(2Mf_{RF}) \tag{61.23}$$

where M is the total number of hypotheses. The expression of shifting NCA in the mth hypothesis is

$$\begin{aligned} S_{3,C}(i,m) &= \sum_{n=1}^{N_{nc}} S_2\left(i - \left[\left[\Delta f_{D,c,m}(n-1)T_{coh}/\tau_s\right]\right],\ n\right) \\ &= \sum_{n=1}^{N_{nc}} R\left(\Delta\tau(i,m,n), T_{coh}, \Delta f_{D,c}\right) \end{aligned} \tag{61.24}$$

where

$$\Delta\tau(i,m,n) = \Delta\tau_i - \tau_s T_c\left[\left[\Delta f_{D,c,m}(n-1)T_{coh}/\tau_s\right]\right] + (n-1)\Delta f_{D,c}T_{coh}/f_c \tag{61.25}$$

After the two-stage of compensation, the distribution of final RCOD $\Delta f'_{D,c}$ is

$$\Delta f'_{D,c} \sim U\left[-\Delta f_D f_c/(2Mf_{RF}),\quad \Delta f_D f_c/(2Mf_{RF})\right] \tag{61.26}$$

By Eqs. (61.18) and (61.26) we know that the longest T_{PIT} supported by method C is M times as long as that supported by method A and B.

If the maximum value of $S_{3,C}(i,m)$ exceeds the detection threshold, which means a successful acquisition, the corresponding $\Delta f_{D,c,m}$ can be used to adjust the CAD. The formula of adjustment is

$$f_D = \hat{f}_D + \Delta f_{D,c,m} f_{RF}/f_c \tag{61.27}$$

After the adjustment, the accuracy of CAD raises M times as before.

The acquisition scheme of method C is presented in Fig. 61.5, in which the CAD is searched in serial while the code-phase is searched in parallel by employing FFT&IFFT implementation [2].

61.5 Simulation Results

This section is devoted to the performance test for the three methods above.

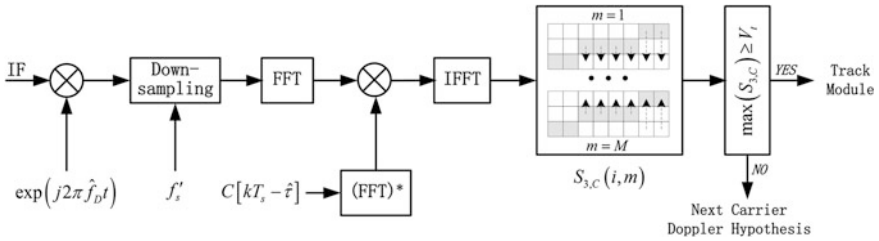

Fig. 61.5 Acquisition scheme of method C

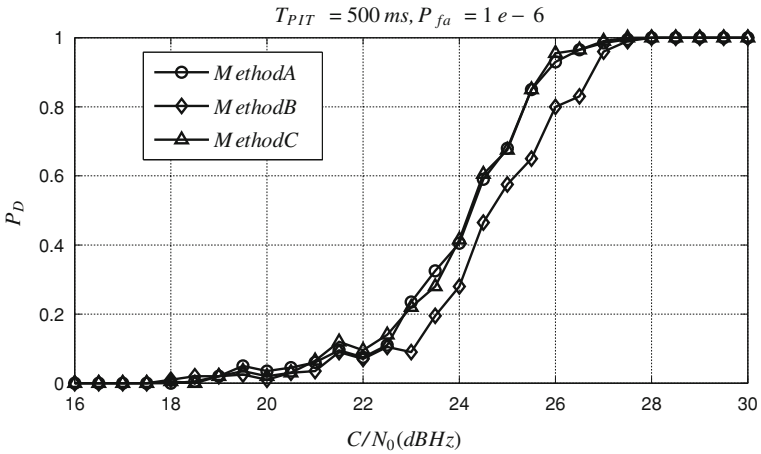

Fig. 61.6 C/N_0 versus P_D for three methods ($T_{PIT} = 500$ ms)

Before the test, an intermediate frequency (IF) signal source is implemented in MATLAB and it can be configured to various parameters. A set of parameters used in this paper are as follows: GPS L1 P-code signal; SV = 5; $f_D = 5.2$ kHz; $p_0 = 9000.5$ chip; $f_{IF} = 46.42$ MHz; $f_s = 62$ MHz; $C/N_0 = 16 \sim 30$ dBHz.

The acquisition parameters used by method A–C are identical and as follows: the search range of code-phase is ± 1 ms with a step of 0.5 chip; the search scope of CAD is ± 6 kHz with a step of 400 Hz; $T_{coh} = 1$ ms; $N_{nc} = 500$ or 1,000; V_t is calculated by Eq. (61.10) when $P_{fa} = 1e-6$. Furthermore, for method C, $M = 5$ in Eq. (61.23).

Every method is tested 200 times under each C/N_0. Figures 61.6 and 61.7 present the curves of C/N_0 versus P_D for method A–C when $T_{PIT} = 500$ ms and $T_{PIT} = 1$ s, respectively.

As we can see from Fig. 61.6, the acquisition sensitivity of method B is about 0.5 dB lower than method A and C. This part of sensitivity loss is caused by the rounding operation in Eq. (61.19). The sensitivities of method A and C are nearly

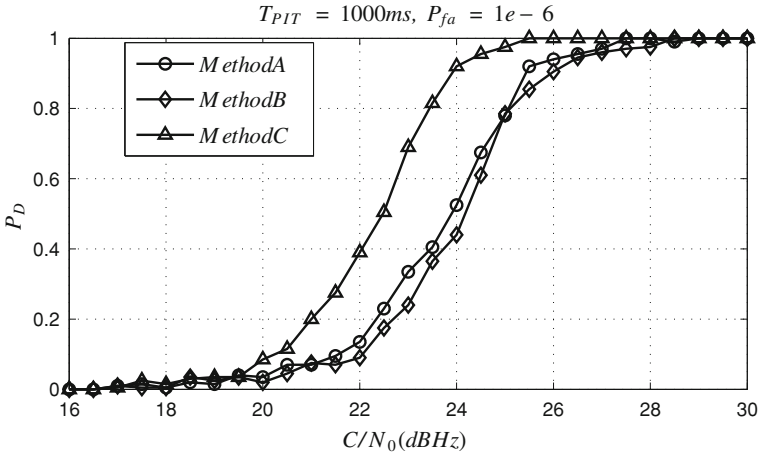

Fig. 61.7 C/N_0 versus P_D for three methods (T_{PIT} = 1,000 ms)

Table 61.1 Maximum amount of FFT and IFFT operations for three methods

Compensation methods	FFT	IFFT
Method A	$(N_{nc} + 2N_{nc}T_{\max}/T_{coh})N_{dl}$	$2N_{nc}T_{\max}/T_{coh}N_{dl}$
Method B	$N_{nc}N_{dl} + 2N_{nc}T_{\max}/T_{coh}$	$2N_{nc}T_{\max}/T_{coh}N_{dl}$
Method C	$N_{nc}N_{dl} + 2N_{nc}T_{\max}/T_{coh}$	$2N_{nc}T_{\max}/T_{coh}N_{dl}$

equal, which means the peak attenuation caused by the RCOD is still relatively small when $T_{PIT} = 500$ ms.

In Fig. 61.7, after the extension of T_{PIT} from 500 ms to 1 s, the acquisition sensitivities of method A and method B both improve only about 0.2 dB, while method C improves about 2 dB. The different improvements of sensitivity illustrate that, as the extension of T_{PIT}, the RCOD becomes the bottleneck of sensitivity improvement. Method C compensates the RCOD, so it achieves a higher sensitivity.

For the search of CAD, results reported by method A and B are 5 kHz, while result from Method C is 5.16 kHz after the adjustment in Eq. (61.27), which is closer to the true value of 5.2 kHz.

Table 61.1 lists the maximum amount of FFT and IFFT operations needed for capturing a satellite. In Table 61.1, N_{dl} is the amount of CAD frequencies being searched, and $T_{\max}$ is the half amount of the searched code-phases. By substituting the acquisition parameters into Table 61.1, it can be drawn that method B and C have the same calculation, which is only 51.27 percent of that needed in method A.

From the above simulation results, a conclusion is made that among the three tested methods, method C obtains the lowest calculation, the highest acquisition sensitivity, and the highest search accuracy of CAD.

61.6 Conclusion

In this paper the effect of COD on acquisition performance is analyzed and a new method of compensating COD is proposed. By adjusting the down-sampling frequency and testing the RCOD under different hypotheses, the new method supports a very long PIT and especially applies to the weak signal acquisition of GNSS. After the comparison test with the existing methods, it can be proved that the new method not only brings about less calculation and higher sensitivity, but also improves the search accuracy of CAD.

Acknowledgments This work was supported by the National Natural Science Foundation of China (Grant No.61101070) and the National Science Foundation for Post-doctoral Scientists of China (Grant No.201104118).

References

1. MacGougan G (2003) High sensitivity GPS performance analysis in degraded signal environments. Master Thesis, Department of Geomatics Engineering, Univerity of Calgary
2. Xie G (2009) Principles of GPS and receiver design. Publishing House of Electronics Industry, Beijing
3. Li C, Wang F, Guo G (2007) Correlation of PN spread spectrum signal under first-order dynamics. Acta Electronica Sinica 35(9):1789–1793
4. Li H, Zhou H, Lu M, Feng Z (2010) Code-doppler-compensation based direct acquisition method for weak GNSS long PN-code. Scientia Sinica Phys, Mech & Astron 40(5):560–567
5. Su SL, Yen NY, Hsieh SC (1995) Code acquisition of direct-sequence spread spectrum communication with Doppler shift. In: Proceedings of IEEE International Conference on Communications, ICC'95 Seattle, 'Gateway to Globalization' vol 3 pp 1663–1667
6. Chen H (2011) Key technologies research on GPS weak signal acquisition. Master Thesis, University of Electronic Science and Technology of China
7. Zhang M, Li G, Zhu Q (2009) Application of doppler frequency compensation algorithm in acquisition of GPS signals. Comput Simul 26(10):69–72
8. Cheng U, Hurd WJ, Statman JI (1990) Spread-spectrum code acquisition in the presence of doppler shift and data modulation. IEEE Trans Commun 38(5):241–250